# Generation of X-ray and Ion Threat Spectra for the Fusion Test Facility Using the BUCKY 1-D Radiation Hydrodynamics Code

T.A. Heltemes, G.A. Moses

November 2006

UWFDM-1315

Presented at the 17th ANS Topical Meeting on Fusion Energy, 13-15 November 2006, Albuquerque NM.

FUSION TECHNOLOGY INSTITUTE

UNIVERSITY OF WISCONSIN

MADISON WISCONSIN

# Generation of X-ray and Ion Threat Spectra for the Fusion Test Facility Using the BUCKY 1-D Radiation Hydrodynamics Code

T.A. Heltemes, G.A. Moses

Fusion Technology Institute
University of Wisconsin
1500 Engineering Drive
Madison, WI 53706

http://fti.neep.wisc.edu

November 2006

UWFDM-1315

Presented at the 17th ANS Topical Meeting on Fusion Energy, 13-15 November 2006, Albuquerque NM.

## Generation of X-ray and Ion Threat Spectra for the Fusion Test Facility Using the BUCKY 1-D Radiation Hydrodynamics Code

T.A. Heltemes[1], G.A. Moses[1]

[1]*University of Wisconsin Fusion Technology Institute: 1500 Engineering Drive, Madison, WI, 53706, taheltemes@wisc.edu*

*The BUCKY 1-D simulation code was used to simulate the hydrodynamic compression and thermonuclear ignition of a DT filled capsule that mimics the specifications set forth by the Fusion Test Facility (FTF) working group. This paper focuses on two key aspects of the ongoing hydrodynamics simulation work being performed at the University of Wisconsin.*

*The first set of simulations was performed to obtain a baseline result for comparison. This baseline utilized the High Average Power Laser (HAPL) target ion and X-ray threat spectra scaled down from 365 MJ to 29.75 MJ. The second set of simulations was a target simulation initiated from conditions that were expected to be found at the point of ignition of the FTF DT target.*

*The results of these simulations allowed for the creation of time-dependent X-ray and ion threat spectra, which will be used in future chamber simulations in support of the FTF design effort to assess the thermal response of test modules located within the facility.*

### I. Introduction

The Fusion Test Facility (FTF) is a laser-driven inertial confinement fusion (ICF) facility which will subject experimental modules to the neutron threat spectrum comparable to that which will be found during operation of the High Average Power Laser (HAPL) ICF power reactor. The FTF consists of a 5 m reaction chamber in which test modules are placed at radial distances of 1 m and 2 m from the center. The FTF will ignite direct-drive DT targets at a rate of 5–10 Hz with a total yield of 29.75 MJ per target (Ref. 1).

A fundamental question of interest to the project is whether or not the test modules can be made robust enough to withstand the ion, X-ray and neutron threat spectra generated by the FTF DT target. One proposed solution to enhance the survivability of the test modules is to coat the plasma-facing surface of the module with an armor material to mitigate the thermal loads generated by the impinging threat spectra.

To assess the effect of adding an armor material to the plasma-facing side of the test modules, the BUCKY 1-D radiation hydrodynamics code (Ref. 2) was used to estimate the transient heating on two candidate armor materials: tungsten and silicon carbide. Simulations were performed at the specified radii of 1 and 2 m from the center of the DT target for each material.

### II. Simulation Setup

### II.A. Chamber Parameters

The FTF modules were simulated as xenon gas-filled chambers with radii of 1 m and 2 m to represent the inner and outer test modules, respectively. The thickness of both armor materials (tungsten and silicon carbide) was set to 1 cm. The chamber was filled with a 66.7 mPa (0.5 mTorr) xenon buffer gas and the entire chamber (gas and armor) has an initial temperature of 600˚C.

The equations of state for the xenon and armor materials in the gas and plasma states were modeled using one-temperature SESAME data (Ref. 3). YAC local thermodynamic equilibrium (LTE) X-ray opacity data were used for the xenon and armor materials (Ref. 4).

Fig. 1 shows the temperature-dependent thermal conductivity of tungsten and silicon carbide. Fig. 2 shows the temperature-dependent specific heat of tungsten and silicon carbide. Dashed values are a linear extrapolation of the last available data point for each quantity.

### II.B. Scaled HAPL Direct-drive Threat Spectra

The first set of simulations use the ion and X-ray threat spectra emanating from the 365 MJ palladium- and

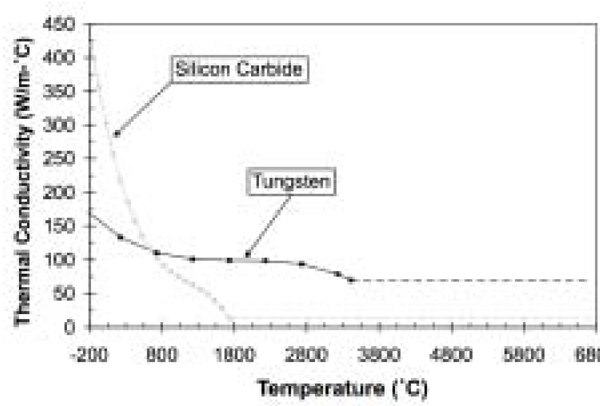


Fig. 1. Thermal conductivity of tungsten and silicon carbide.

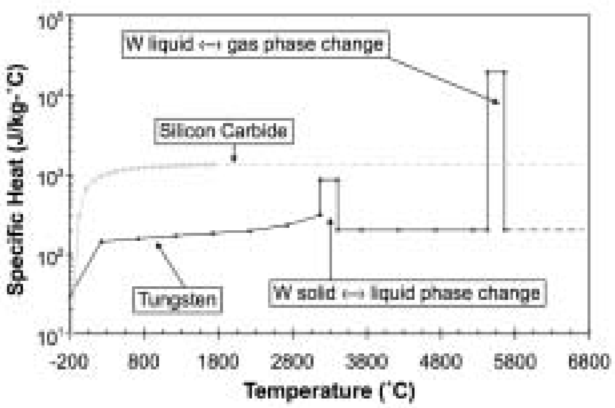

Fig. 2. Specific heat of tungsten and silicon carbide.

gold-coated HAPL target. A LASNEX simulation performed at Lawrence Livermore National Laboratory (LLNL) was used to obtain the HAPL target spectra, which were reported as time-integrated values at 100 ns (Ref. 5).

The HAPL ion and X-ray threat spectra were reduced to values appropriate to the FTF target by using a linear scaling factor of the ratio of the two target yields

$$\alpha = 365 / 29.75 \approx 0.0815 . \quad (1)$$

The ions were launched at $t = 0$ s and the X-ray time dependence was built back into the simulation by scaling the spectra with a 170 ps full-width half-maximum (FWHM) Gaussian function from $t = 0$ s to $t = 750$ ps. The total yield of the scaled HAPL target is 29.75 MJ from the following yields: (1) a charged particle yield of 6.99 MJ, (2) a neutron yield of 22.36 MJ, and (3) an X-ray yield of 0.40 MJ.

**II.C. BUCKY Compressed FTF Target Threat Spectra**

The scaled HAPL target simulations are based on the assumption that the yields from the FTF direct-drive target scale linearly from the full-scale HAPL direct-drive target. This assumption may not be valid due to the differences in relative masses of the material layers — the plastic coating and palladium/gold overcoat being the materials of greatest relative difference.

The FTF target radial build as injected into the FTF chamber is shown in Fig. 3, which will be referred to in this paper as the cold FTF target (Ref. 6). BUCKY was used to perform a simulation of the 365 MJ HAPL target up to the point of ignition. Temperature, density and zone velocity values for the HAPL target were used to construct the FTF target at the point just prior to thermonuclear ignition. Two additional criteria were used to ensure that the target would ignite and burn to the proper yield: (1) the center of the DT target would contain a hot spot with $\rho R = 0.4$ g/cm$^3$ and (2) temperature of

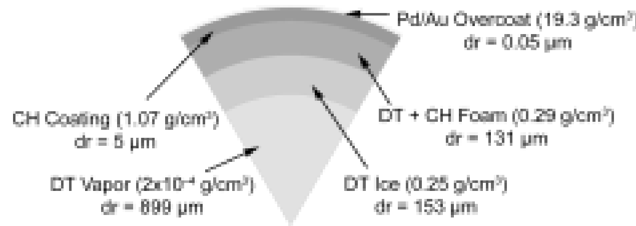

Fig. 3. Cold FTF target radial build.

4.0 keV. Table I shows the numerical values for temperature and velocity (negative values denote zones moving toward the center of the target) used as initial conditions in the compressed FTF target and Fig. 4 shows the compressed FTF target radial build. It should be noted that there was no equation-of-state or X-ray opacity data available for the palladium and gold mixture, a layer of pure gold was used instead. The BUCKY simulation used a global temperature boundary of 1 eV and pressure boundary of 66.7 mPa (0.5 mTorr). All materials in the BUCKY simulation used SESAME equations of state and YAC LTE X-ray opacities.

**III. BUCKY Simulation Results**

**III.A. BUCKY Compressed FTF Target Yield**

The compressed FTF target BUCKY simulation produced a total yield of 28.0 MJ from the following yields: (1) a charged particle yield of 5.0 MJ, (2) a neutron yield of 20.1 MJ, and (3) an X-ray yield of

TABLE I. Compressed FTF Target Initial Conditions

| Compressed FTF Target Region | Initial Temperature (eV) | Initial Zone Velocity (cm/s) |
|---|---|---|
| DT “Hot Spot” | 4000 | $-6.4\times10^7$ |
| DT | 800 | $-6.4\times10^7$ |
| DT+CH | 600 | $6.4\times10^7$ |
| CH | 400 | $6.4\times10^7$ |
| Au | 200 | $6.4\times10^7$ |

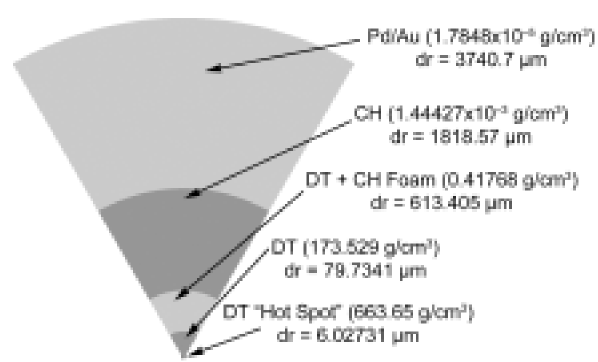

Fig. 4. Compressed FTF target radial build.

2.9 MJ. The FWHM of the X-ray pulse was 24 ps and the FWHM of the charged particle and neutron pulse was 22 ps. Fig. 5 shows the combined charged particle and neutron yield and power, fig. 6 shows the X-ray yield and power during the simulation. The simulation was run to 10 ns to ensure that the ablating gold zones did not exceed 1 m from the center of the target.

### III.B. HAPL scaled-target and Compressed FTF target Spectra Comparison

Fig. 7 shows the X-ray spectra for the scaled HAPL target and the FTF target. Fig. 8 shows the proton and deuteron spectra for the scaled HAPL target and the FTF target. Fig. 9 shows the tritium and helium-4 spectra for the scaled HAPL target and the FTF target. Fig. 10 shows the carbon and gold spectra for the scaled HAPL target and the FTF target.

It was noted that the compressed FTF target produces ion threat spectra with a much narrower energy distribution and overall lower ion threat spectrum energy compared to the scaled HAPL ion threat spectra. This is believed to be due to the lower energy scales (driver and yield) of the FTF target compared to the full-scale HAPL target. The gold ions show much higher energies than that of the scaled HAPL target spectrum. This is believed to be due to a numerical artifact in the BUCKY code that over-accelerates the ions expanding into a vacuum or near

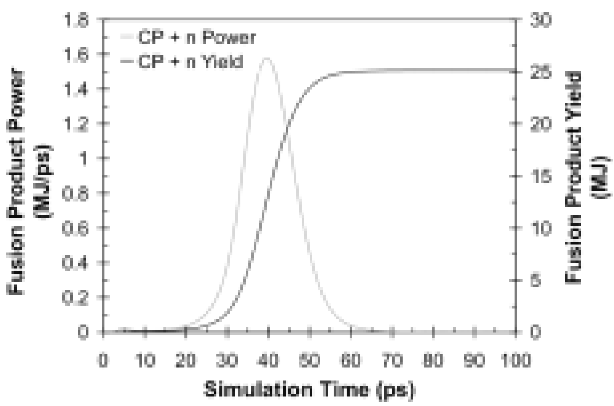


Fig. 5. Fusion product (charged particles plus neutrons) yield (right axis) and power (left axis) from the compressed FTF target simulation.

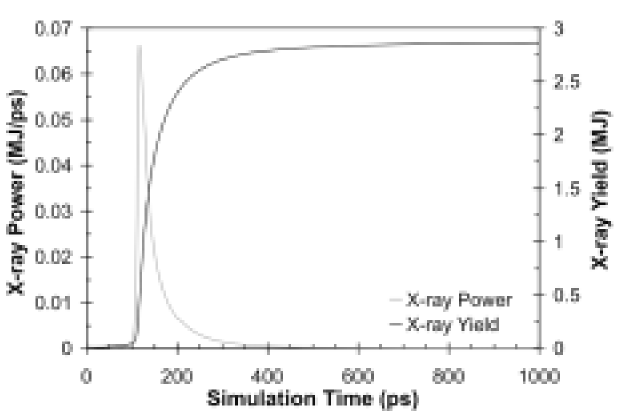


Fig. 6. X-ray yield (right axis) and power (left axis) from the compressed FTF target simulation.

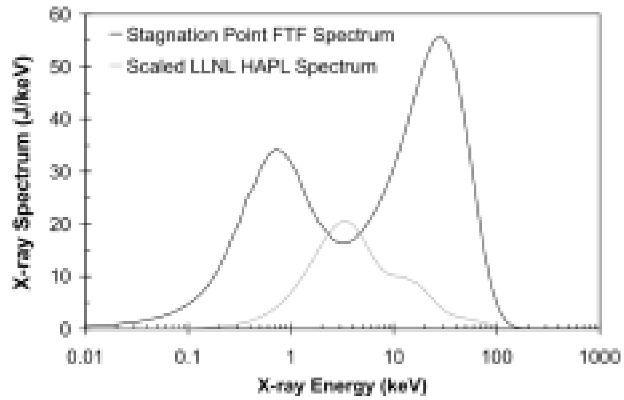


Fig. 7. X-ray spectra from the scaled HAPL and compressed FTF targets.

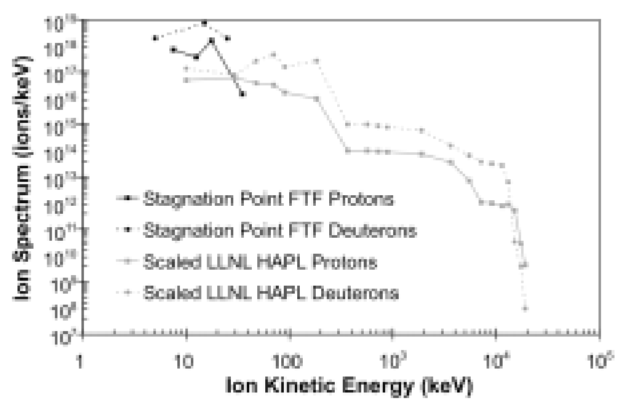


Fig. 8. Hydrogen and deuterium ion spectra from the scaled HAPL and compressed FTF targets.

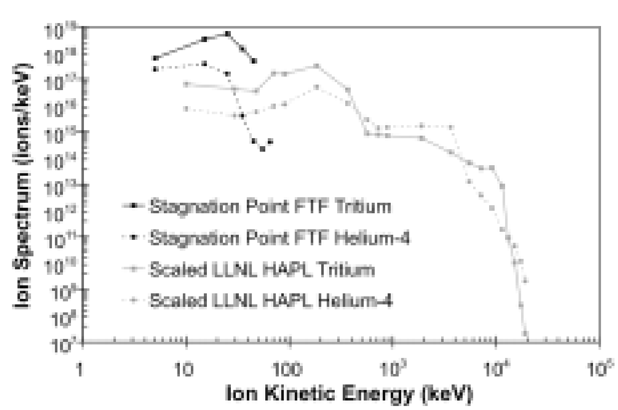


Fig. 9. Tritium and Helium spectra from the scaled HAPL and compressed FTF targets.

vacuum region.

The results of the comparison indicate that there may not be a linear scaling relationship between the HAPL 365 MJ direct-drive target and the FTF direct-drive target. Table II demonstrates this by comparing some fundamental target parameters per unit mass of the target. This is not a conclusive result, however. The BUCKY simulations used LTE X-ray opacities everywhere. This is believed to cause BUCKY to overestimate the X-ray yield from the gold region of the FTF target. Future simulations will employ non-LTE X-ray opacity data for gold to more accurately reflect X-ray transport and heating through the gold plasma ablating from the target.

### III.C. Temperature Rise on the Plasma-facing Surface of the Test Modules

The scaled HAPL target and FTF target ion and X-ray threat spectra were used as source terms for the chamber simulations described in Section II.A. The temperature of the armor in a 100 nm layer at the plasma-facing surface was recorded. All ions were launched at $t$ = 0s and the X-ray spectra were temporally scaled by a Gaussian function with a FWHM of 170 ps for the scaled HAPL target and 24 ps for the compressed FTF target.

Fig. 11 shows the surface temperature of the 1 m test module with tungsten armor. Fig. 12 shows the surface temperature of the 2 m test module with tungsten armor. Fig. 13 shows the surface temperature of the 1 m test module with silicon carbide armor. Fig 14 shows the surface temperature of the 2 m module with silicon carbide armor. It was noted that for both the scaled HAPL target and the FTF target ion and X-ray threat spectra, the 1 m tungsten module melted under the X-ray deposition in the armor. The compressed FTF target simulation for the 1 m target shows that the surface of the module in fact reaches the vaporization temperature of the material, but the 100 nm armor layer does not ablate. Silicon carbide surface temperatures appear to be low enough to serve as adequate protection for the test modules at either 1 m or

TABLE II. HAPL and FTF direct-drive target comparison

| Parameter | HAPL 365 MJ Target | FTF 29.75 MJ Target |
|---|---|---|
| Target Total Mass (mg) | 8.002 | 1.167 |
| Specific Driver Energy (MJ/mg) | 0.307 | 0.428 |
| Specific Target Gain (1/mg) | 18.533 | 25.493 |
| Specific Charged Particle Yield (MJ/mg) | 10.979 | 4.287 |
| Specific Neutron Yield (MJ/mg) | 34.279 | 17.244 |
| Specific X-ray Yield (MJ/mg) | 0.617 | 2.472 |
| Specific X-ray pulse FWHM (ps/mg) | 21.2 | 20.6 |
| Specific Total Yield (MJ/mg) | 45.625 | 25.493 |

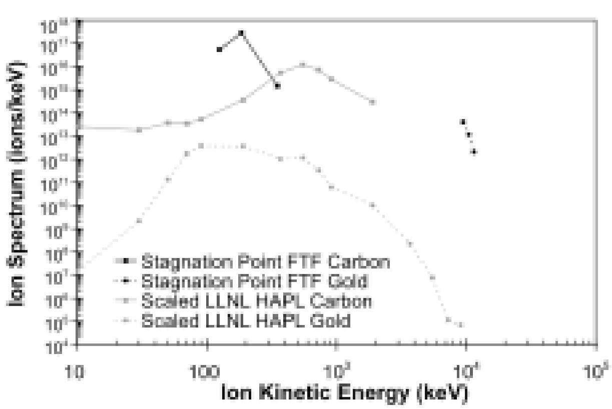


Fig. 10. Carbon and gold ion spectra from the scaled HAPL and compressed FTF targets.

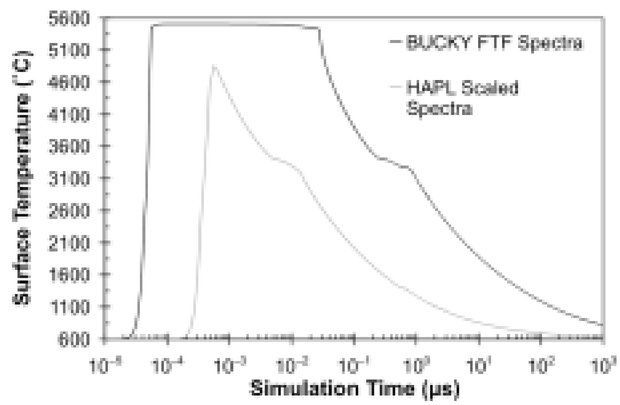


Fig. 11. Surface temperature of the tungsten armored 1 m test module for the scaled HAPL and compressed FTF X-ray and ion threat spectra.

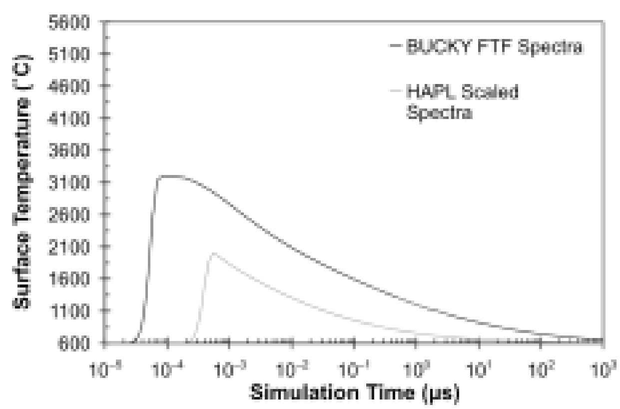


Fig. 12. Surface temperature of the tungsten armored 2 m test module for the scaled HAPL and compressed FTF X-ray and ion threat spectra.

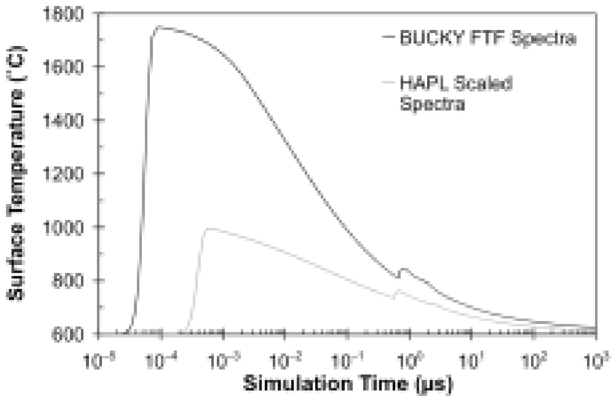


Fig. 13. Surface temperature of the silicon carbide armored 1 m test module for the scaled HAPL and compressed FTF X-ray and ion threat spectra.

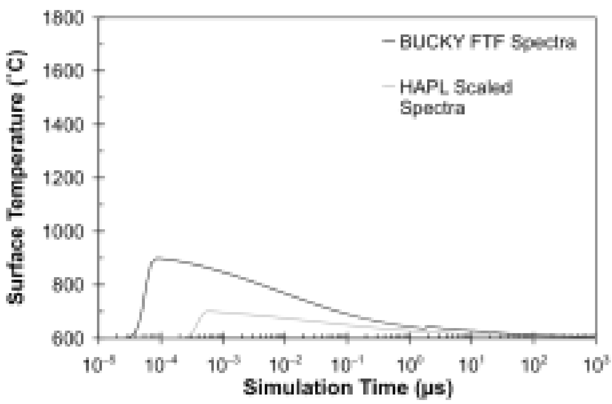


Fig. 14. Surface temperature of the silicon carbide armored 2 m test module for the scaled HAPL and compressed FTF X-ray and ion threat spectra.

2 m from the center of the reaction chamber.

## IV. CONCLUSIONS

X-ray and ion threat spectra for the FTF direct-drive DT target were estimated using two methods: (1) a linear scaling of the spectra from the 365 MJ direct-drive HAPL target, and (2) using a BUCKY simulation of the proposed FTF target near the point of thermonuclear ignition. Results of the BUCKY simulations indicate that it may not be appropriate to linearly scale the HAPL target yield to serve as a surrogate for the FTF ion and X-ray threat spectra. The BUCKY results are preliminary and improved modeling of the X-ray opacities in the gold region will need to be implemented to obtain more accurate threat spectra.

The surface heating results from both sets of ion and X-ray spectra indicate that tungsten is not an appropriate armor material for the 1 m test module, but should provide sufficient thermal protection for the 2 m test module. Silicon carbide appears to provide adequate thermal protection for the test modules at both 1 m and 2 m from the center of the reaction chamber.

## ACKNOWLEDGMENTS

This work was supported in part by a grant from the Naval Research Laboratory, award no. N00173-01-1-G012. The authors wish to thank Dr. Robert R. Peterson of Los Alamos National Lab for his assistance with the BUCKY simulation of the 365 MJ full-scale HAPL target.

## REFERENCES

1. S. P. Obenschain, D. G. Colombant, A. J. Schmitt, J. D. Sethian, and M. W. McGeoch, “Pathway to a lower cost high repetition rate ignition facility,” *Phys. Plasmas* **13**, 056320 (2006).
2. R.R. Peterson, J.J. MacFarlane, G.A. Moses, “BUKCY—A 1-D Radiation Hydrodynamics Code for Simulating Inertial Confinement Fusion High Energy Density Plasmas,” *UWFDM-984*, University of Wisconsin (1995).
3. B. I. Bennet, J. D. Johnson, G. I. Kerley, and G. T. Rood, “Recent Developments in the SESAME Equation-of-State Library,” Los Alamos National Laboratory, NM, *LA-7130* (1978).
4. J. Yuan, D.A. Haynes, R.R. Peterson, G.A. Moses, “Flexible database-driven opacity and spectrum calculations,” *J. Quant. Spect. Rad. Trans.* **81**, 513 (2003).
5. Available online at http://www.aries.ucsd.edu/HAPL/DOCS/HAPLtargetSpecs.pdf
6. Private communication with NRL, May (2006).